Nonlinearity

Branches and bifurcations of ejection–collision orbits in the planar circular restricted three body problem

OPEN ACCESS
IOP Publishing | London Mathematical Society Nonlinearity
Nonlinearity **38** (2025) 045010 (25pp) https://doi.org/10.1088/1361-6544/adbda3

Branches and bifurcations of ejection–collision orbits in the planar circular restricted three body problem

Gianni Arioli[1,3] **and J D Mireles James**[2,4,*]

[1] Department of Mathematics, Politecnico di Milano, Milan, Italy
[2] Department of Mathematics & Statistics, Florida Atlantic University, Boca Raton, FL, United States of America

E-mail: jmirelesjames@fau.edu and gianni.arioli@polimi.it

Received 17 January 2024; revised 15 January 2025
Accepted for publication 6 March 2025
Published 13 March 2025

Recommended by Dr Hinke M Osinga

Abstract

The goal of this paper it to prove existence theorems for one parameter families (branches) of ejection-collision orbits in the planar circular restricted three body problem (CRTBP), and to study some of bifurcations of these branches. The CRTBP considers the dynamics of an infinitesimal particle moving in the gravitational field of two massive primary bodies. The motion of the primaries assumed to be circular, and we study ejection–collision orbits where the infinitesimal body is ejected from one primary and collides with the other (as opposed to more local ejections–collisions where the infinitesimal body collides with a single primary body in both forward and backward time). We consider branches of ejection–collision orbits which are (i) parameterized by the Jacobi integral (energy like quantity conserved by the CRTBP) with the masses of the primaries fixed, and (ii) parameterized by the mass ratio of the primary bodies with energy fixed. The method of proof is constructive and computer assisted, hence can be applied in non-perturbative settings and (potentially) to other conservative systems of differential equations. The main requirement is

[3] G A partially supported by PRIN project 2022 'Partial differential equations and related geometric-functional inequalities', financially supported by the EU, in the framework of the 'Next Generation EU initiative'.
[4] J M J partially supported by NSF grant DMS - 2307987.
* Author to whom any correspondence should be addressed.

that the system should admit a change of coordinates which regularizes the collision singularities. In the planar CRTBP, the necessary regularization is provided by the classical Levi–Civita transformation.

Keywords: three body problem, ejection–collision,
Levi–Civita regularization, continuation-bifurcation, computer assisted proof

Mathematics Subject Classification numbers: 37M20, 70F16, 65G40, 70F07

1. Introduction

Collisions are an essential feature of celestial mechanics problems, and the scourge of global dynamics. This is because, given the initial positions and velocities of a collection of N gravitating point masses, collisions obstruct the extension of local solution curves throughout all time. It is then a fundamental question to determine the embedding of the forward collision manifold: that is, the set of all initial conditions which reach collision in finite forward time. The backward collision manifold, or ejection manifold, is defined similarly by considering backwards time evolution.

Despite intense of work on the problem over nothing less than centuries, the collision manifold is completely understood in only the simplest cases. For example the case of two bodies, which reduces to the Kepler problem, and a few other completely integrable systems. An illuminating discussion of the state-of-the art for $N = 3$ bodies is found in the introduction of the paper by Guardia *et al* [1], where they prove a kind of density result for the collision manifold in a perturbative regime where two of the three bodies are very small.

One fruitful approach which provides valuable partial results is to focus on the complement of the collision manifold, and to study the properties of orbits whose global existence is assumed *a-priori*. A capstone example of this strategy is the celebrated classification theorem of Chazy, published in 1922 [2], describing the possible forward/backward asymptotic time behavior of all collision-free orbits in the three body problem. See again [1] for a precise statement of Chazy's theorem in modern language, and for a thorough discussion of the surrounding literature.

Another, more constructive approach is to to study invariant sets like relative equilibria, relative periodic orbits, relative invariant tori, and heteroclinic/homoclinic connections between these (*relative* invariance here refers to solutions studied in an appropriate rotating frame). Moreover, given one of these invariant objects it is typically possible to develop a normal form describing the dynamics nearby. This approach has deep roots in Poincaré's groundbreaking New Methods [3–5]. From the point of view of collisions, orbits lying in fully invariant sets are necessarily collision-free, and hence in the complement of both the ejection and collision manifolds.

An antipodal, but equally constructive approach is to study the (local) collision manifold using techniques of regularization. The idea of regularizing three body collisions goes back (at least) to the work of Levi–Civita in the 1920s [6], and we refer to Chapter three Szebehely's book [7], and to the lecture notes of Celletti [8] for more on the historical development of regularization and many additional references. The main point, from the perspective of the present discussion, is that regularizing coordinate transformations replace collision sets with well defined geometric objects which can be advected or 'grown' using the regularized flow. Further away from these regularized geometric objects, the local representation can be transformed back to the original coordinates and advected further. In this light, collision manifolds

are similar to local stable/unstable manifolds attached to invariant objects, and exhibit all the complexity which Poincaré himself complained was 'difficult to draw'.

Rather than study the full complexity of the ejection and collision manifolds, one can mimic the approach of dynamics systems theory and study only their intersections. These intersections give rise to 'connecting orbits' which we refer to as ejection–collision orbits. Ejection–collision orbits where the same two bodies collide in forward and backward time are referred to as 'homoclinic', and have been studies extensively from both perturbative and numerical view points. We refer the interested reader to the works of Ollé, *et al* [9, 10] and to Ollé *et al* [11] for powerful existence results, numerical simulations, and detailed discussion of the literature. See also the introduction of [12], discussed further below.

Another, more global situation is when a body A collides with a body B in backward time but with a different body C in forward time. We refer to such orbits as ejection–collision heteroclinics, and they are the focus of the present work.

Analytical results for ejection–collision heteroclinics in the three body problem are found in Llibre, and Llibre and Lacomba [13, 14]. Their arguments are perturbative, with the rotating Kepler problem serving as the unperturbed system, and the masses of the second and third bodies along with the reciprocal of energy as small parameters. In lay terms, their result shows that an energetic enough particle aimed at the Moon from the Earth can strike it.

For larger mass ratios and/or lower energies, purely analytic techniques falter. Numerical computations come to the rescue and, when mathematical rigor is desired, techniques from validated numerics (for example interval arithmetic) can be combined with *a-posteriori*, Newton–Kantorovich type analysis to construct existence arguments. This is a part of what is called *computer-assisted proof in analysis*, and some remarks about the literature are given in appendix. In the present work, we develop computer assisted existence results for parameter dependent families of heteroclinic ejection–collision orbits in the planar circular restricted three body problem (CRTBP).

The CRTBP was introduced by Poincaré as a simplified model of three body dynamics, and we recall the equations of motion in section 2. Briefly, the problem studies—in a co-rotating frame—the dynamics of an infinitesimal particle moving in the vicinity of two massive primary bodies (think of a man-made satellite or comet) . The primary bodies are assumed to evolve on Keplerian circles, and to be unaffected by the presence of the infinitesimal third body. Again, an excellent general reference remains the book of Szebehely [7], with a more modern treatment being the book of Meryer *et al* [15]. See figure 1 for a schematic illustration of the CRTBP. Example results obtained using our methods are illustrated in figures 2 and 3, with detailed descriptions found in section 3.

We note that the the recent work of Capiński, Kepley, and the second deals with computer assisted proofs for collision and near collision orbits in the CRTBP with energy and mass parameters fixed [12]. Additional comments about the differences between [12] and the present work are found in appendix. We also mention a recent preprint by Capiński and Pasiut [16] which applies techniques based on those of [12] to prove the existence of a horseshoe-like invariant set where orbits pass arbitrarily close to collision infinitely many times in the Earth–Moon CRTBP.

Finally we note that, because our computer assisted arguments are built on top of accurate numerical approximations of one parameter branches of ejection–collision orbits in the CRTBP, our work is closely related (and deeply indebted) to classical numerical continuation and bifurcation theory: especially to the literature on computation and continuation of invariant objects in celestial mechanics. This literature in this area is vast, going all the way back to the work of Darwin [17], Strömgren [18] and Moulton *et al* [19] at the turn of the Twentieth Century. A thorough review of this literature is a task far beyond the scope of the present

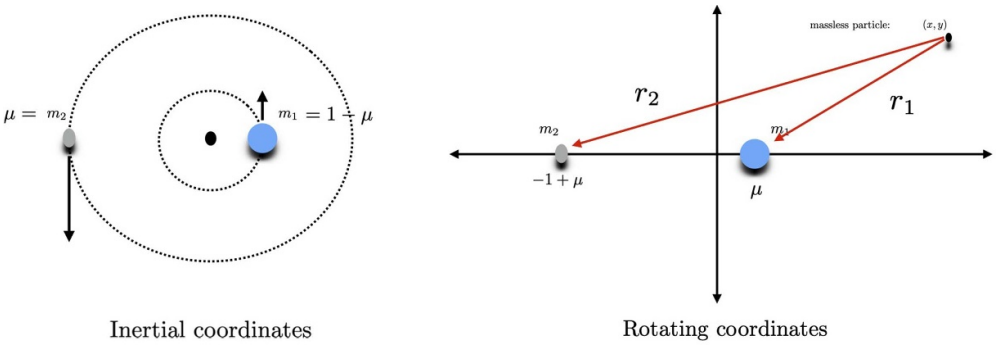

Figure 1. Configuration of the circular restricted three body problem: the left frame illustrates the motion of the massive primary bodies m_1 and m_2 in inertial coordinates. The are restricted *a-priori* to Keplerean circles. The line determined by the position of m_1, m_2 and the center of mass rotates at a constant speed, and it is possible to change to a co-rotating coordinate system with constant angular velocity, thus removing the motion of primaries. Inserting a massless test particle into the resulting gravitational vortex, one obtains the CRTBP as illustrated in the right frame.

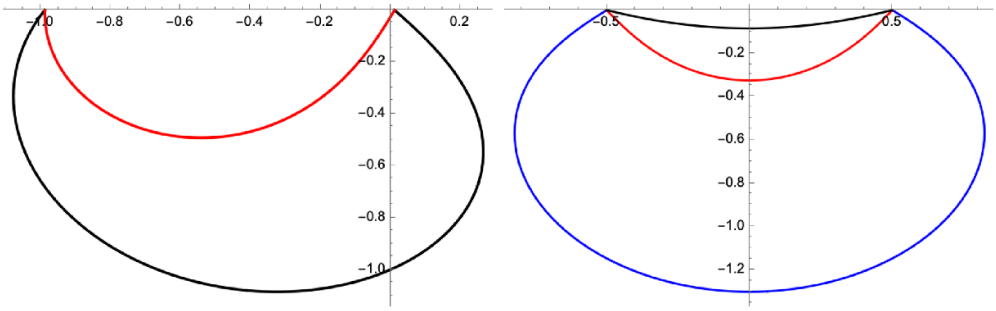

Figure 2. Branches parameterized by energy: the 5 approximate heteroclinic ejection–collision orbits form the statement of theorem 1. The left frame illustrates trajectories 1 (black) and 2 (red) in the Earth–Moon system, while the right frame illustrates trajectories 3 (black), 4 (red), and 5 (blue) in the equal mass (or Copenhagen) system.

work, and we refer to the works of Muñoz-Almaraz *et al* [20], Doedel *et al* [21], Doedel *et al* [22], and Calleja *et al* [23] for detailed descriptions of numerical continuation techniques for branches of invariant objects in the CRTBP. By consulting these Papers, and the references therein, the reader will obtain an much clearer picture of the wider literature. More general references include the Lecture notes of Simo [24] and of Doedel [25], as well as the book of Kuznetsov [26].

The remainder of the paper is organized as follows. In section 2 we recall the equations of motion for the CRTBP, as well as the coordinate changes and the resulting regularized equations of motion resulting from the Levi–Civita transformations. section 3 states precisely our main results, and in section 4 we describe the formulation of the fixed point problem for the boundary value problems (BVPs) used to study ejection–collision orbits. In section 5 we present the appropriate bifurcation theory for branches of solutions to the BVPs discussed in section 4, and in section 6 we discuss the *a-posteriori* analysis for branches of such solutions. Finally, in section 7 we discuss some implementation details for the computer assisted proofs.

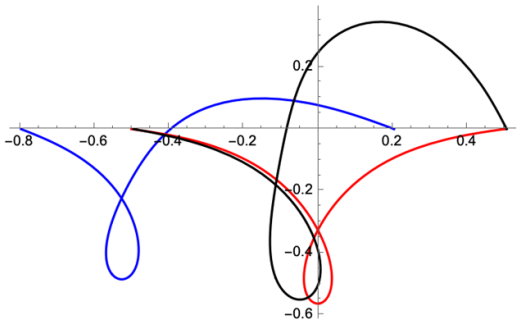

Figure 3. A global branch of heteroclinic ejection–collision orbits parameterized by mass ratio: the figure illustrates some approximate orbits from theorem 2. We note that, in the CRTBP, the mass parameter μ is normalized so that it lies in the interval $[0,1/2]$. This branch starts a $\mu = 1/2$, decreases to $\mu = \mu_* < 1/2$, undergoes a fold bifurcation, and returns to $\mu = 1/2$: hence we follow it over its full lifespan. The blue curve illustrates the solution at the bifurcation parameter (mass ratio) $\mu = \mu^*$, while the red and black the solutions at $\mu = 1/2$. the figure illustrates the result of theorem 2, which shows that there exists a one parameter family of ejection–collision orbits, parameterized by μ, which connects the red to the black solution through the saddle node bifurcation at the blue solution. Note that for the orbits in this family, the radial velocity with respect to the large primary vanishes twice, hence the family is dynamically different from the one established in [13].

In particular, we describe computer assisted verification of the hypotheses of the *a-posteriori* theorems developed earlier in the paper. Appendix provides a few additional remarks about the surrounding literature.

2. The planar CRTBP

Let m_1 and m_2 denote the masses of the primary bodies. We assume that $m_1 \geqslant m_2$, and define the mass ratio

$$\mu = \frac{m_2}{m_1 + m_2}.$$

Note that $\mu \in [0,1/2]$, with $\mu = 0$ when $m_2 = 0$ and $\mu = 1/2$ when $m_1 = m_2$.

Consider

$$\gamma' = f_\mu(\gamma), \tag{1}$$

where $\gamma = (x,p,y,q)$, and f_μ is the one parameter family of vector fields given by

$$f_\mu(x,p,y,q) := \begin{pmatrix} p \\ 2q + x - \frac{(1-\mu)(x-\mu)}{r_1^3} - \frac{\mu(x+1-\mu)}{r_2^3} \\ q \\ -2p + y - \frac{(1-\mu)y}{r_1^3} - \frac{\mu y}{r_2^3} \end{pmatrix}. \tag{2}$$

Here

$$r_1 = \sqrt{(x-\mu)^2 + y^2}, \qquad \text{and} \qquad r_2 = \sqrt{(x+1-\mu)^2 + y^2}.$$

We refer to the ordinary differential equation given by equation (1) as the planar circular restricted three body problem or CRTBP, and remark that when $\mu = 0$ the system reduces to the rotating Kepler problem. This is the key to perturbative approaches to the problem, but will play no role in the present work.

Equation (1) is derived, starting from Newton's laws for three massive gravitating bodies, by assuming the motion of the primary bodies is known and circular, and that the mass of the third body goes to zero. One then changes to a rotating frame revolving with the frequency of the primaries based at their center of mass. Equation (1) is obtained after choosing units of distance, mass, and time so that the primaries (whose locations are fixed in by the rotating frame) have coordinates $(x_1, y_1) = (\mu, 0)$ and $(x_2, y_2) = (-1+\mu, 0)$, and so that the masses become $m_1 = 1-\mu$ and $m_2 = \mu$. A schematic illustration of the configuration space is seen in the right frame of figure 1.

Orbits of the massless particle—that is, solutions of the differential equation (1) - conserve the scalar quantity

$$E(x,p,y,q) = -p^2 - q^2 + 2\Omega(x,y), \tag{3}$$

where

$$\Omega(x,y) = (1-\mu)\left(\frac{r_1^2}{2} + \frac{1}{r_1}\right) + \mu\left(\frac{r_2^2}{2} + \frac{1}{r_2}\right).$$

The function E defined in equation (3) is referred to as the Jacobi integral or Jacobi constant and sometimes, in a slight abuse of terminology, we refer to E as the energy of the system.

We now define the two dimensional affine subsets of $\mathbb{R}^4$ given by

$$\mathcal{C}_\mu^1 = \left\{(x,p,y,q) \in \mathbb{R}^4 \,|\, x = \mu \text{ and } y = 0\right\},$$

and

$$\mathcal{C}_\mu^2 = \left\{(x,p,y,q) \in \mathbb{R}^4 \,|\, x = -1+\mu \text{ and } y = 0\right\}.$$

These are the singular sets associated with the positions of the first and second primary bodies respectively. They correspond to the situation where the position of the massless particle coincides with the position of one of the primaries: that is, a collision.

Let

$$\mathcal{C}_\mu = \mathcal{C}_\mu^1 \cup \mathcal{C}_\mu^2,$$

and note that

$$U_\mu = \mathbb{R}^4 \backslash \mathcal{C}_\mu, \tag{4}$$

is the natural domain of f_μ. In this paper we focus on $\mu \in (0, 1/2]$, as the case of $m_2 = \mu = 0$ degenerates to the rotating Kepler problem, and the singularity associated with the second primary vanishes. In this case no ejection from or collision with the second primary is possible.

We note that, since f_μ is locally Lipschitz on U_μ (in fact real analytic), we have that the orbit of every initial condition $\gamma(0) \in U_\mu$ either exists for all time, or else accumulates to $\mathcal{C}_\mu$ in finite time. We refer to $\mathcal{C}_\mu$ as *the collision set*, and say that an orbit which accumulates to $\mathcal{C}_\mu$ in finite forward time is a *collision orbit*. Similarly, an orbit which accumulates to $\mathcal{C}_\mu$ in finite backward time is referred to as an *ejection orbit*. Finally, an orbit which accumulates to $\mathcal{C}_\mu$ in

both finite forward and finite backward time is an *ejection–collision orbit*, and the objects of our study.

To formalize these notions, let $\pi : \mathbb{R}^4 \to \mathbb{R}^2$ be the projection onto position variables given by

$$\pi\,(x,p,y,q) = (x,y)\,.$$

We make the following definition.

Definition 1 (Ejection–collisions). Let $T_1 \in (-\infty,0)$, $T_2 \in (0,\infty)$ and $\mu \in (0,1/2]$. We say that the curve $\gamma\colon (T_1,T_2) \to U_\mu \subset \mathbb{R}^4$ is an m_1 to m_2 ejection–collision orbit if

$$\frac{\mathrm{d}}{\mathrm{d}t}\gamma(t) = f_\mu\left(\gamma(t)\right),$$

for $t \in (T_1,T_2)$, and

$$\lim_{t\to T_1} \pi\gamma(t) = (\mu,0)\,, \qquad \text{and} \qquad \lim_{t\to T_2} \pi\gamma(t) = (-1+\mu,0)\,.$$

The energy of the ejection–collision orbit is

$$E(\gamma(0)) = C.$$

If the limits are reversed then γ is an m_2 to m_1 ejection–collision orbit.

To understand velocity as the infinitesimal body approaches collision, consider $\gamma\colon (T_1,T_2) \to U_\mu \subset \mathbb{R}^4$ an m_1 to m_2 ejection–collision orbit in the sense of definition 1. We claim that a collision is in fact just a certain kind of finite time blow up. To see this, let $v(t) = \sqrt{p(t)^2+q(t)^2}$ denote the magnitude of velocity. (The discussion is easily modified for m_2 to m_1 ejection–collisions). The energy of the orbit is $C = E(\gamma(0))$, and we write

$$\gamma(t) = \begin{pmatrix} x(t) \\ p(t) \\ y(t) \\ q(t) \end{pmatrix},$$

to denote the components of the orbit. In particular, since γ is an m_1 to m_2 ejection–collision we have that

$$\lim_{t\to T_1} x(t) = -1+\mu, \qquad \text{and} \qquad \lim_{t\to T_2} x(t) = -\mu,$$

so that

$$\lim_{t\to T_1} r_1(t) = \lim_{t\to T_2} r_2(t) = 0. \tag{5}$$

(These are swapped if γ is m_2 to m_1).

Recalling equation (3), we now have that

$$C = -v(t)^2 + 2\Omega\left(x(t),y(t)\right),$$

where

$$\Omega\left(x\left(t\right),y\left(t\right)\right)=\left(1-\mu\right)\left(\frac{r_1\left(t\right)^2}{2}+\frac{1}{r_1\left(t\right)}\right)+\mu\left(\frac{r_2\left(t\right)^2}{2}+\frac{1}{r_2\left(t\right)}\right).$$

It follows from equation (5) that $\Omega(x(t),y(t))\to\infty$ as $t\to T_{1,2}$, and since

$$v\left(t\right)^2=2\Omega\left(x\left(t\right),y\left(t\right)\right)-C,$$

with C constant, we have that

$$v\left(t\right)\to\pm\infty,\qquad\qquad\text{as } t\to T_{1,2}.$$

That is, at least one of $p(t)$ or $q(t)$ becomes infinite as the infinitesimal body approaches collision. One concludes that orbits accumulate to $C^{1,2}_{\mu}$ only at infinity.

2.1. Regularized coordinates for collisions with m_1

We now review the classical Levi–Civita transformations [6], which allow us to extend orbits of the CRTBP up to and through collision. We state a number of standard results without proof, and refer again to [7, 8] for more details.

To regularize a collision with m_1, write $z=x+\mathrm{i}y$ and define new regularized variables $\hat{z}=\hat{x}+\mathrm{i}\hat{y}$. These are related to z by the transformation

$$\hat{z}^2=z-\mu.$$

It is also necessary to rescale time in the new coordinates according to the formula

$$\frac{\mathrm{d}t}{\mathrm{d}\hat{t}}=4|\hat{z}|^2.$$

Next one fixes a value c of the Jacobi constant and, a standard calculation (see [7]), transforms the vector field f of equation (2) to the regularized Levi–Civita vector field $f_1^c\colon U_1\to\mathbb{R}^4$ given by

$$f_1^c\left(\hat{x},\hat{p},\hat{y},\hat{q}\right)=\begin{pmatrix}\hat{p},\\ 8\left(\hat{x}^2+\hat{y}^2\right)\hat{q}+12\hat{x}\left(\hat{x}^2+\hat{y}^2\right)^2+16\mu\hat{x}^3+4\left(\mu-c\right)\hat{x}+\frac{8\mu\left(\hat{x}^3-3\hat{x}\hat{y}^2+\hat{x}\right)}{\left(\left(\hat{x}^2+\hat{y}^2\right)^2+1+2\left(\hat{x}^2-\hat{y}^2\right)\right)^{3/2}},\\ \hat{q},\\ -8\left(\hat{x}^2+\hat{y}^2\right)\hat{p}+12\hat{y}\left(\hat{x}^2+\hat{y}^2\right)^2-16\mu\hat{y}^3+4\left(\mu-c\right)\hat{y}+\frac{8\mu\left(-\hat{y}^3+3\hat{x}^2\hat{y}+\hat{y}\right)}{\left(\left(\hat{x}^2+\hat{y}^2\right)^2+1+2\left(\hat{x}^2-\hat{y}^2\right)\right)^{3/2}}\end{pmatrix}. \tag{6}$$

Note that the open set $U_1\in\mathbb{R}^4$ defined by

$$U_1=\left\{\hat{\mathrm{x}}=(\hat{x},\hat{p},\hat{y},\hat{q})\in\mathbb{R}^4:(\hat{x},\hat{y})\notin\left\{(0,-1),(0,1)\right\}\right\},$$

serves as the domain of the regularized system, that the regularized vector field is well defined at the origin $(\hat{x},\hat{y})=(0,0)$, and that the origin is mapped to the collision with m_1 when inverting the Levi–Civita coordinate transformation. A schematic illustration of the regularized configuration space is given in the bottom right frame of figure 4.

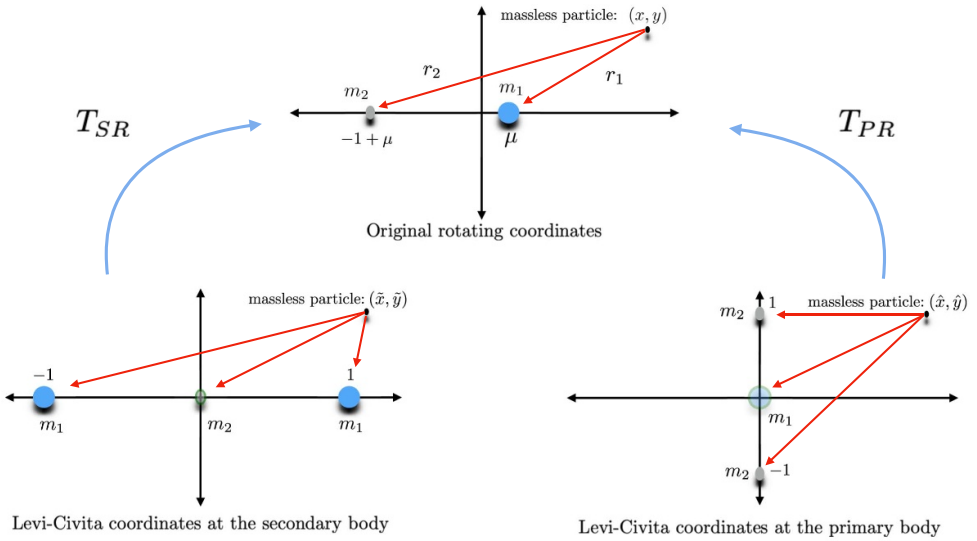

Figure 4. Levi–Civita regularized coordinates: center top figure depicts the configuration space of the CRTBP, with singularities at $(x,y) = (-1+\mu, 0)$ and at $(x,y) = (\mu, 0)$ due to collision of the massless particle with the smaller primary m_2 or the larger primary m_1 respectively. The bottom left and right figures depict the configuration spaces of the Levi–Civita systems associated with regularization of the smaller and larger masses respectively. Note that in the bottom left and right frames the massive bodies m_2 and m_1 respectively have been moved to the origin. These bodies are depicted as 'ghosts' using transparencies to indicate that the resulting fields are perfectly well defined there. However, the double covering introduced by the complex squaring function creates mirror images of the remaining primary, so that the Levi–Civita systems still have a pair of singular point. These mirrored singular points are located at $(x,y) = (\pm 1, 0)$ for the case the regularization at m_2 and at $(x,y) = (0, \pm 1)$ for the regularization at m_1. The mirrored singularities play no role in our set up, as we employ the Levi–Civita coordinates only in a small neighborhood of the origin.

By working out the change of coordinates for the velocity variables, one defines the coordinate transformation $T_1 \colon U_1 \backslash \mathcal{C}_1 \to U$ between the original and regularized coordinates by

$$\mathrm{x} = T_1(\hat{\mathrm{x}}) := \begin{pmatrix} \hat{x}^2 - \hat{y}^2 + \mu \\ \frac{\hat{x}\hat{p} - \hat{y}\hat{q}}{2(\hat{x}^2+\hat{y}^2)} \\ 2\hat{x}\hat{y} \\ \frac{\hat{y}\hat{p} + \hat{x}\hat{q}}{2(\hat{x}^2+\hat{y}^2)} \end{pmatrix}. \tag{7}$$

Note that T_1 is a local diffeomorphism on $U_1 \backslash \mathcal{C}_1$. The regularized vector field conserves the first integral $E_1^c \colon U_1 \to \mathbb{R}$ given by

$$E_1^c(\hat{\mathbf{x}}) = -\hat{q}^2 - \hat{p}^2 + 4\left(\hat{x}^2+\hat{y}^2\right)^3 + 8\mu\left(\hat{x}^4-\hat{y}^4\right) + 4(\mu-c)\left(\hat{x}^2+\hat{y}^2\right) + 8(1-\mu) + 8\mu\frac{\left(\hat{x}^2+\hat{y}^2\right)}{\sqrt{\left(\hat{x}^2+\hat{y}^2\right)^2+1+2\left(\hat{x}^2-\hat{y}^2\right)}}. \tag{8}$$

An essential point is that the fixed energy parameter c appears in f_1^c and E_1^c as a parameter. We remark that a point with energy c in the original coordinate system is transformed to a point with energy zero in the regularized coordinates. Then, since collision in the original coordinates corresponds to the origin in the regularized coordinates, the intersection of the collision set with the zero energy level set is given by

$$E_1^c(0,\hat{p},0,\hat{q}) = -\hat{q}^2 - \hat{p}^2 + 8(1-\mu) = 0,$$

or

$$\hat{q}^2 + \hat{p}^2 = 8(1-\mu). \tag{9}$$

That is the the Levi–Civita transformation maps the intersection of the collision set $\mathcal{C}_\mu^1$ with the energy level set $E=c$ to the origin cross the velocity circle given in equation (9).

2.2. Regularized coordinates for collisions with m_2

In a precisely analogous way, one can regularize collisions with the second primary as follows. Write $\tilde{z} = \tilde{x} + \mathrm{i}\tilde{y}$, define $\tilde{z}^2 = z + 1 - \mu$, rescale time as $\mathrm{d}t/\mathrm{d}\tilde{t} = 4|\tilde{z}|^2$, and fix an energy level c in the original coordinates. Another lengthy calculation results in the regularized field $f_2^c : U_2 \to \mathbb{R}^4$ defined as

$$f_2^c(\tilde{x},\tilde{p},\tilde{y},\tilde{q}) = \begin{pmatrix} \tilde{p} \\ 8\left(\tilde{x}^2+\tilde{y}^2\right)\tilde{q} + 12\tilde{x}\left(\tilde{x}^2+\tilde{y}^2\right)^2 - 16(1-\mu)\tilde{x}^3 + 4((1-\mu)-c)\tilde{x} + \frac{8(1-\mu)\left(-\tilde{x}^3+3\tilde{x}\tilde{y}^2+\tilde{x}\right)}{\left((\tilde{x}^2+\tilde{y}^2)^2+1+2(\tilde{y}^2-\tilde{x}^2)\right)^{3/2}} \\ \tilde{q} \\ -8\left(\tilde{u}^2+\tilde{y}^2\right)\tilde{p} + 12\tilde{y}\left(\tilde{x}^2+\tilde{y}^2\right)^2 + 16(1-\mu)\tilde{y}^3 + 4((1-\mu)-c)\tilde{y} + \frac{8(1-\mu)\left(\tilde{y}^3-3\tilde{x}^2\tilde{y}+\tilde{y}\right)}{\left((\tilde{x}^2+\tilde{y}^2)^2+1+2(\tilde{y}^2-\tilde{x}^2)\right)^{3/2}} \end{pmatrix} \tag{10}$$

defined on the domain

$$U_2 := \mathbb{R}^4 \backslash \mathcal{C}_2 = \left\{\tilde{\mathrm{x}} = (\tilde{x},\tilde{p},\tilde{y},\tilde{q}) \in \mathbb{R}^4 \,|\, (\tilde{x},\tilde{y}) \notin \{(-1,0),(1,0)\}\right\}, \qquad \text{where}$$
$$\mathcal{C}_2 := \left\{\tilde{\mathrm{x}} = (\tilde{x},\tilde{p},\tilde{y},\tilde{q}) \in \mathbb{R}^4 \,|\, \tilde{x} = \tilde{y} = 0\right\}.$$

The complete change of coordinates is given by

$$\mathbf{x} = T_2(\tilde{\mathrm{x}}) = \begin{pmatrix} \tilde{x}^2 - \tilde{y}^2 + \mu - 1 \\ \frac{\tilde{x}\tilde{p}-\tilde{y}\tilde{q}}{2\left(\tilde{x}^2+\tilde{y}^2\right)} \\ 2\tilde{x}\tilde{y} \\ \frac{\tilde{y}\tilde{p}+\tilde{x}\tilde{q}}{2\left(\tilde{x}^2+\tilde{y}^2\right)} \end{pmatrix}. \tag{11}$$

A schematic illustration of the configuration space is given in the bottom left frame of figure 4.

We also remark that system conserves the scalar quantity

$$E_2^c(\tilde{\mathbf{x}}) = -\tilde{p}^2 - \tilde{q}^2 + 4\left(\tilde{x}^2+\tilde{y}^2\right)^3 + 8(1-\mu)\left(\tilde{y}^4-\tilde{x}^4\right) + 4\left((1-\mu)-c\right)\left(\tilde{x}^2+\tilde{y}^2\right) + 8(1-\mu)\frac{\tilde{x}^2+\tilde{y}^2}{\sqrt{\left(\tilde{x}^2+\tilde{y}^2\right)^2+1+2\left(\tilde{y}^2-\tilde{x}^2\right)}} + 8\mu, \tag{12}$$

so that, arguing as in the previous section, the intersection of the collision set $\mathcal{C}_\mu^2$ with the c energy level set is given by the product of the origin and the circle

$$\tilde{p}^2 + \tilde{q}^2 = 8\mu. \tag{13}$$

3. Statement of the main results

We now describe our main results. The goal of the remainder of present work is to prove the following theorems.

Theorem 1. *For each pair of parameter values (μ, C) given in below table, there exists an $m_1 = 1-\mu$ to $m_2 = \mu$ ejection–collision orbit at energy level C. Solutions 3,4,5 are symmetric with respect to $x \mapsto -x$, see figure 2.*

Solution	μ	C
1	μ_{em}	2
2	μ_{em}	$845 \times 2^{-9} \approx 1.65$
3	1/2	-6
4	1/2	2
5	1/2	2

Having established the existence of ejection–collision orbits as illustrated in theorem 1, our next task is to ask wether such orbits persist as the energy or mass ratio is varied. The next three theorems, which constitute the main results of the present work, deal with branches of ejection–collision orbits from one primary to the other, and bifurcations of such branches. We consider two kinds of branches: those parameterized by energy with mass ratio held fixed, and those parameterized by mass ratio with energy fixed. For example we have the following.

Theorem 2. *For $C_* = 205 \times 2^{-6} \approx 3.203$, there exists*

$$\mu_* \in [3261, 3263] \times 2^{-14} \qquad (\textit{that is } \mu_* \approx 0.1991),$$

and two distinct branches of m_2 to m_1 ejection–collision orbits parameterized by $\mu \in [\mu_*, 1/2]$ and energy C_*. The two branches are real analytic on $(\mu_*, 1/2]$ and terminate in a saddle node bifurcation at μ_*.

The next theorem establishes the existence of a one parameter branch of ejection–collision orbits, parameterized by energy, in the Copenhagen problem. That is, the CRTBP with $\mu = 1/2$ (equal masses). The results of the theorem are illustrated in figure 5.

Theorem 3. *For $\mu = 1/2$, there exist*

$$C_* = 2163799 \times 2^{-20} \qquad (\textit{that is } C_* \approx 2.063559532),$$

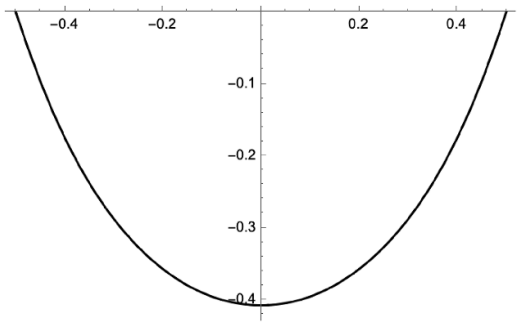

Figure 5. Approximate orbits in the configuration space in rotating coordinates of the solution at C^* obtained by theorem 3. For this family the radial velocity with respect to the first primary does not vanish, hence it is related to the family of [13]. However, theorem 3 holds at the highly non-perturbative energy of $\mu = 1/2$.

and

$$C^* \in [8453, 8454] \times 2^{-12}, \qquad (\textit{that is } C^* \approx 2.06372),$$

and two distinct branches of m_1 to m_2 ejection–collision orbits for $f_{1/2}$ parameterized by $C \in [C_*, C^*]$. The branches are real analytic on (C_*, C^*) and terminate in a saddle node bifurcation at C^*.

The last theorem is similar, but for the Earth/Moon problem. That is, the CRTBP with $\mu = \mu_{em} \stackrel{\text{def}}{=} 13256063 \times 2^{-30} \approx 0.012345\,67$. The results of the theorem are illustrated in figure 6.

Theorem 4. *For $\mu_{em} \stackrel{\text{def}}{=} 13256063 \times 2^{-30} \approx 0.012345\,67$, there exist*

$$C_* = 34395443031 \times 2^{-34} \qquad (\textit{that is } C_* \approx 2.002078284916933\,6259),$$

and

$$C^* \in \left(34395443031 \times 2^{-34}, 34395443369 \times 2^{-34}\right),$$

and two distinct branches of m_1 to m_2 ejection-collision orbits for $f_{\mu_{em}}$ parameterized by $C \in [C_*, C^*]$. The two branches are real analytic on (C_*, C^*) and terminate in a saddle node bifurcation at C^*.

4. The fixed point equation

In this section we formulate a fixed point problem $\mathcal{F}(X) = X$ whose solution corresponds to an ejection–collision orbit in the CRTBP. The main idea is to reformulate definition 1 in terms of the observations discussed in section 2. Again, the overall strategy is to approximately solve the fixed point equation using numerical methods, and then to construct a Newton–Kantorovich type argument in the vicinity of the approximate solution, with the goal of proving the existence of a true solution nearby.

Recall that the vector field defining CRTBP, and both vector fields defining the regularized dynamics in Levi–Civita coordinates, are real analytic on their domains of definition. See

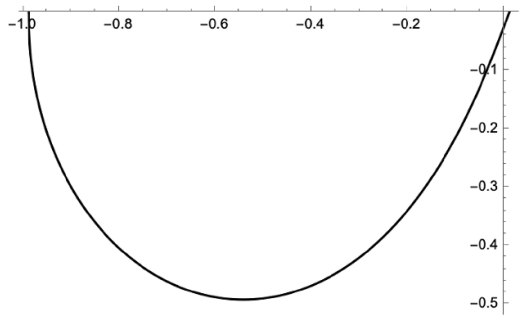

Figure 6. Approximate orbits in the configuration space in rotating coordinates of the solution at C^* obtained by theorem 4. The family is similar to the one established by theorem 3, but for the physically realistic Earth–Moon mass ratio.

equations (2), (6) and (10). Because of this, it is natural to look for real analytic solutions. So, for $\varrho, \rho > 0$ define

$$\mathcal{A}_\rho \stackrel{\text{def}}{=} \left\{ z : [-1,1] \to \mathbb{R} : z(t) = \sum_{j\geqslant 0} z_j t^j \,, \sum_{j\geqslant 0} |z_j| \rho^j < +\infty \right\}, \tag{14}$$

and

$$\mathcal{B}_\varrho \stackrel{\text{def}}{=} \left\{ z : [-1,1] \to \mathbb{R} : z(t) = \sum_{j\geqslant 0} z_j T_j(t) \,, \sum_{j\geqslant 0} |z_j| \varrho^j < +\infty \right\}. \tag{15}$$

Here $\{z_j\} \subset \mathbb{R}$ and T_j denotes the jth Chebyshev polynomial. These sets define Banach spaces (Banach algebras even) when endowed with the norms

$$\|z\|_{\mathcal{A}} \stackrel{\text{def}}{=} \sum_{j\geqslant 0} |z_j| \rho^j \,, \qquad \|z\|_{\mathcal{B}} \stackrel{\text{def}}{=} \sum_{j\geqslant 0} |z_j| \varrho^j,$$

and consist of real valued functions with analytic extensions to the complex unit disk of radius ρ in the case of $\mathcal{A}_\rho$, or to the complex ellipse with foci $\{-1,1\}$ and semiaxes $\frac{1}{2}(\varrho + \varrho^{-1})$ where $\frac{1}{2}(\varrho - \varrho^{-1})$ in the case of $\mathcal{B}_\varrho$.

To study ejection–collision orbits from m_1 to m_2 we write $(x_1(t), p_1(t), y_1(t), q_1(t))$ to denote orbit segments in the Levi–Civita coordinates regularized at m_1, $(x_2(t), p_2(t), y_2(t), q_2(t))$ for orbit segments in the coordinates regularized at m_2, and $(x_0(t), p_0(t), y_0(t), q_0(t))$, to denote orbit segments in the original coordinates. We write T_1, T_2, and T_0 to denote the time spent in each these coordinate system (where T_1 and T_2 are measured in regularized units of time).

We use Taylor series expansions to describe orbit segments in regularized coordinates, and Chebyshev series expansions in the original rotating coordinates. This choice is motivated by the idea that we will take a small time step in the regularized coordinates whose purpose is to move us away from collision, and then spend the remaining time in the original rotating frame. Then in general T_0 may be substantially larger than T_1, T_2, and we use Chebyshev series to describe the longer orbit segment. We rescale time so that $[0, T_1]$ and $[0, T_2]$ become $[0,1]$, and $[0, T_0]$ becomes $[-1,1]$, as these are natural domains for Taylor and Chebyshev series expansions respectively.

The ejection–collision orbit is then a solution of the following constrained BVP:

$$\begin{cases} \dot{p}_1 = T_1 f_1(x_1, y_1, p_1, q_1) \\ \dot{q}_1 = T_1 g_1(x_1, y_1, p_1, q_1) \\ \dot{p}_0 = T_0 f_0(x_0, y_0, p_0, q_0) \\ \dot{q}_0 = T_0 g_0(x_0, y_0, p_0, q_0) \\ \dot{p}_2 = T_2 f_2(x_2, y_2, p_2, q_2) \\ \dot{q}_2 = T_2 g_2(x_2, y_2, p_2, q_2) \\ \dot{x}_i = T_i p_i, \quad i = 0,1,2 \\ \dot{y}_i = T_i q_i, \quad i = 0,1,2 \\ x_1(0) = 0 \\ y_1(0) = 0 \\ p_1(0)^2 + q_1(0)^2 = 8(1-\mu), \\ T_{PR}(x_1(1), p_1(1), y_1(1), q_1(1)) = (x_0(-1), p_0(-1), y_0(-1), q_0(-1)), \\ T_{SR}(x_2(-1), p_2(-1), y_2(-1), q_2(-1)) = (x_0(1), p_0(1), y_0(1), q_0(1)), \\ x_2(0) = 0 \\ y_2(0) = 0 \\ p_2(0)^2 + q_2(0)^2 = 8\mu, \end{cases} \tag{16}$$

where $f_{1,2}, g_{1,2}$ are the second and fourth components of the functions $f^c{}_i$ defined by equations (6) and (10) respectively, and f_0, g_0 are the second and fourth components of the CRTB vector field defined in equation (2). Note that the equations $p_1(0)^2 + q_1(0)^2 = 8(1-\mu)$ and $p_2(0)^2 + q_2(0)^2 = 8\mu$ impose that the orbit segments in regularized coordinates begin or end with collision at the correct Jacobi level, as discussed in sections 2.1 and 2.2. The transformations T_{PR} and T_{SR} insure that the endpoints of the regularized orbit segments match the end points of the segment in the standard rotating coordinates.

Now, for $x \in \mathcal{A}_\rho$ (or $\mathcal{B}_\varrho$), we denote by $D_c^{-1}x$ the inverse of the differentiation operator applied to x. We normalize so that the zeroth order Taylor (resp. Chebyshev) coefficient of the result is c. Note that we can choose this coefficient freely, as the zeroth order Chebyshev and Taylor polynomials are constant.

The problem as stated has 14 boundary conditions, however because of conservation of energy, we only need 13 constraints. We choose the parameters as follows. Set

$$\begin{aligned} (d_1, d_2, d_3, d_4) = T_{\mathrm{SR}}(x_2(-1), p_2(-1), y_2(-1), q_2(-1)) \\ - (x_0(1), p_0(1), y_0(1), q_0(1)), \end{aligned} \tag{17}$$

so that four boundary conditions become $d_1 = d_2 = d_3 = d_4 = 0$. Then we choose

- $c_1 = c_2 = c_5 = c_6 = 0$, which imply that $x_1(0) = 0, y_1(0) = 0, x_2(0) = 0, y_2(0) = 0$.
- c_3, c_4, a_0, b_0 in order to satisfy the equality

$$(\hat{x}_0(-1), \hat{p}_0(-1), \hat{y}_0(-1), \hat{q}_0(-1)) = T_{\mathrm{PR}}(x_1(1), p_1(1), y_1(1), q_1(1)).$$

- $a_1 = p_1(0) + d_2$
- $a_2 = p_2(0) + d_3$
- $b_1 = \pm\sqrt{8(1-\mu) - p_1^2(0)}$
- $b_2 = \pm\sqrt{8\mu - p_2^2(0)}$.

Observe that we have to know in advance whether $q_1(0)$ and $q_2(0)$ are positive or negative, in order to choose the correct sign for b_1 and b_2. These choices are determined from the numerical approximation of the solution we are trying to validate.

We are ready to define the maps $\mathcal{X} = \mathcal{A}^8 \times \mathcal{B}^4 \times \mathbb{R}$ and $\mathcal{F} : \mathcal{X} \to \mathcal{X}$ by

$$\begin{aligned}&\mathcal{F}(x_1, y_1, x_0, y_0, x_2, y_2, p_1, q_1, p_0, q_0, p_2, q_2, T_0)\\ &\quad = \left(\tilde{x}_1, \tilde{y}_1, \tilde{x}_0, \tilde{y}_0, \tilde{x}_2, \tilde{y}_2, \tilde{p}_1, \tilde{q}_1, \tilde{p}_0, \tilde{q}_0, \tilde{p}_2, \tilde{q}_2, \tilde{T}_0\right)\end{aligned} \tag{18}$$

where

$$\begin{cases}(\tilde{x}_1, \tilde{y}_1, \tilde{x}_0, \tilde{y}_0, \tilde{x}_2, \tilde{y}_2) = D_{c_i}^{-1}(T_1 p_1, T_1 q_1, T_0 p_0, T_0 q_0, T_2 p_2, T_2 q_2)\\ \tilde{p}_1 = T_1 D_{a_1}^{-1} f_1(x_1, y_1, p_1, q_1)\\ \tilde{q}_1 = T_1 D_{b_1}^{-1} g_1(x_1, y_1, p_1, q_1)\\ \tilde{p}_0 = T_0 D_{a_0}^{-1} f_0(x_0, y_0, p_0, q_0)\\ \tilde{q}_0 = T_0 D_{b_0}^{-1} g_0(x_0, y_0, p_0, q_0)\\ \tilde{p}_2 = T_2 D_{a_2}^{-1} f_2(x_2, y_2, p_2, q_2)\\ \tilde{q}_2 = T_2 D_{b_2}^{-1} g_2(x_2, y_2, p_2, q_2)\\ \tilde{T}_0 = T_0 + d_4\,,\end{cases} \tag{19}$$

and the constants $\{a_i, b_i, c_i, d_i\}$ are chosen as described above. It is straightforward to check that a fixed point X of $\mathcal{F}$ corresponds to an ejection–collision solution; in particular $d_2 = d_3 = d_4 = 0$, and because of the conservation of energy $d_1 = 0$ as well. Note also that a solution of this equation is continuous and *a-priori* piecewise analytic, thanks to the decay rates imposed by the norms on the sequence spaces. Moreover, since the CRTBP vector field of equation (2) is real analytic on its domain of definition, the entire ejection–collision solution curve—when projected back into rotating coordinates—is globally analytic up to the singularities at the endpoints.

5. Fixed point problem for studying the bifurcations

We begin by discussing the local analysis near the bifurcation points appearing in theorems 2–4. The argument is based on a procedure introduced in [27], which we now briefly review. Note that the map $\mathcal{F}$ defined in equation (18) depends on the parameters μ and C, through the component functions $f_{0,1,2}$, $g_{0,1,2}$ of the vector fields defined in equations (2), (6) and (10). We will vary one or the other of these parameters, which we refer to as τ. More precisely, $\tau = C$ in theorems 3 and 4, while $\tau = \mu$ in theorem 2.

We write $\mathcal{F}_\tau$ to stress the explicit dependence of the map on the chosen parameter and, in a slight abuse of notation, define $\mathcal{F} : \mathbb{R} \times \mathcal{X} \to \mathcal{X}$ by

$$\mathcal{F}(\tau, X) = \mathcal{F}_\tau(X) - X. \tag{20}$$

Then, for a fixed value of τ, X_τ is an ejection–collision orbit with system parameter τ if and only if $\mathcal{F}(\tau, X_\tau) = 0$. We write either $X(\tau)$ or X_τ depending on whether we wish to stress that X is a function of τ, or a branch of solutions parameterized by τ.

Our goal is to numerically approximate the parameter value τ_* where a bifurcation occurs, and then to validate that there is a true bifurcation nearby via a contraction mapping argument. We also need mathematically rigorous bounds on the local branch(es) near the bifurcation point. Our strategy is to develop a kind of normal form $g(\tau,\lambda)$ for the fixed point operator $\mathcal{F}_\tau$, in such a way that the zero level set of g describes the branch in a neighborhood of the numerically computed bifurcation point.

To formalize the discussion, we begin with a two-parameter family of functions $X(\tau,\lambda)$ solving

$$(\mathbb{I}-\ell)\,\mathcal{F}\,(\tau,X(\tau,\lambda))=0\,,\qquad \ell X(\tau,\lambda)=\lambda\hat{X}, \tag{21}$$

where $\mathbb{I}$ is the identity map on $\mathcal{X}$, and $\ell:\mathcal{X}\to\mathcal{X}$ is a one-dimensional projection whose image approximates the kernel of $D\mathcal{F}(\tau,X)$, and $\hat{X}\in\mathcal{X}$ is in the range of ℓ. Choose $\{e_j\}_{j\in\mathbb{N}}$ a basis of $\mathcal{X}$, so that each of the functions e_j is in either $\mathcal{A}_\rho$ or $\mathcal{B}_\varrho$ depending on context. Take $\hat{X}=\sum_{j=0}^{N}\hat{X}_j e_j$ an approximate eigenvector of $D\mathcal{F}(\tau,.)$ corresponding to the numerically smallest eigenvalue. We fix the scale by choosing $\hat{X}$ with $\sum_{j=0}^{N}\hat{X}_j^2=1$, and define the projection ℓ by

$$\ell X=\ell_0\,(X)\,\hat{X},\qquad \ell_0\,(u)=\sum_{j=0}^{N}X_j\hat{X}_j. \tag{22}$$

Here X_j are the coefficients of X in the basis $\{e_j\}$.

The goal now is to show that equation (21) has a smooth and locally unique solution $X: I\times J\to\mathcal{X}$ on some rectangle $I\times J$ in the parameter space. Toward this end, define the bifurcation function $g\colon I\times J\to\mathbb{R}$ by

$$g\,(\tau,\lambda)=\ell_0\mathcal{F}\,(\tau,X(\tau,\lambda))\,. \tag{23}$$

We observe that $g(\tau,\lambda)$ is zero when $X(\tau,\lambda)$ is a solution of $\mathcal{F}(\tau,X)=0$.

We expand the coefficients of X (and hence X itself) about the point (τ_0,λ_0) as Taylor polynomials in τ,λ of the form

$$X\,(\tau,\lambda)=\sum_j X_j\,(\tau,\lambda)\,e_j\,,\quad X_j=\sum_{0\leqslant l+m\leqslant M}X_{jlm}\left(\frac{\tau-\tau_0}{\tau_1}\right)^l\left(\frac{\lambda-\lambda_0}{\lambda_1}\right)^m. \tag{24}$$

Here $\tau_0,\tau_1,\lambda_0\lambda_1,M$ are as given in table 1 (note that $\tau=\mu$ in the case $i=1$ and $\tau=C$ in the cases $i=2,3$). We refer to such expansions as $\mathcal{X}-$Taylor or (XT) series in τ and λ, and to the truncations as XT polynomials. Solving equation (21) for the unknown branch $X=X(\tau,\lambda)$ is equivalent to finding a fixed point of the map $\mathcal{F}_{\tau,\lambda}$, defined by

$$\mathcal{F}_{\tau,\lambda}\,(X)=(\mathbb{I}-\ell)\,\mathcal{F}_\tau\,(X)+\lambda\hat{X}. \tag{25}$$

Our goal is to use the Banach fixed point theorem to obtain a true solution near our numerical approximation.

The map $\mathcal{F}$ is not a (local) contraction, but it is compact. More precisely, its derivative $D\mathcal{F}$ has all eigenvalues, but finitely many, of modulus less than 1. To prove the existence of a fixed point of $\mathcal{F}$ by means of the Banach fixed point theorem we define the new mapping

$$\mathcal{G}_{\tau,\lambda}\,(h)=\mathcal{F}_{\tau,\lambda}\,(\bar{X}+\Lambda_{\tau,\lambda}h)-\bar{X}+M_{\tau,\lambda}h\,,\qquad \Lambda_{\tau,\lambda}=\mathbb{I}-M_{T,\lambda}\,, \tag{26}$$

Table 1. Parameters for the bifurcations.

i	τ_0	τ_1	λ_0	λ_1	M
1	$1631\cdot 2^{-13}$	$5\cdot 2^{-14}$	$5\cdot 2^{-7}$	2^{-4}	14
2	$8453\cdot 2^{-12}$	2^{-12}	$51\cdot 2^{-8}$	$25\cdot 2^{-9}$	12
3	$8397325\cdot 2^{-22}$	2^{-26}	$-2102\cdot 2^{-13}$	$3\cdot 2^{-13}$	8

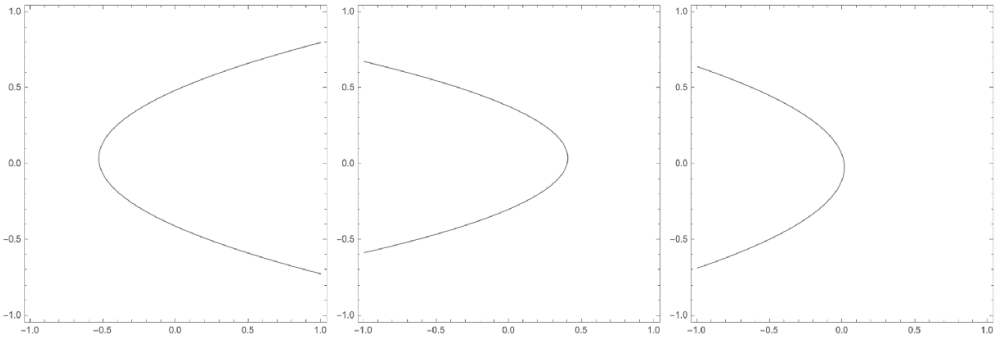

Figure 7. Approximate zero level curve for the functions $g(\tau,\lambda)$ describing the saddle-node bifurcations in theorems 2–4.

where $\bar{X}$ is approximately fixed by $\mathcal{F}_{\tau_0,\lambda_0}$, and $M_{\tau,\lambda}$ is a finite rank operator having that $\Lambda_{\tau,\lambda} = \mathbb{I} - M_{\tau,\lambda}$ approximately inverts the operator $\mathbb{I} - D\mathcal{F}_{\tau_0,\lambda_0}(\bar{X})$, and we observe that, if h is a fixed point for $\mathcal{G}_{\tau,\lambda}$, then $\bar{X} + \Lambda_{\tau,\lambda} h$ is a fixed point for $\mathcal{F}_{\tau,\lambda}$. One can see that any solution, by the implicit function theorem, depends analytically on τ and λ.

Let $D_r(z)$ denote the complex disk of radius r centered at z. We can, with the aid of a computer, prove the following theorem. See section 7 for discussion of the implementation.

Lemma 1. *For $i = 1,2,3$, let $\tau_0,\tau_1,\lambda_0,\lambda_1,M$ as in table 1, define $I = D_{\tau_1}(\tau_0)$ and $J = D_{\lambda_1}(\lambda_0)$. There exists an XT polynomial $\bar{X}(\tau,\lambda)$ as in (24), and positive constants ε, r, K satisfying $\varepsilon + Kr < r$, so that*

$$\|\mathcal{G}_{\tau,\lambda}(0)\| \leqslant \varepsilon, \qquad \|D\mathcal{G}_{\tau,\lambda}(v)\| \leqslant K. \tag{27}$$

for all $v \in B_r(0)$ and all $\tau \in I$, $\lambda \in J$.

Combining the Banach fixed point theorem with lemma 1, we now have the following result:

Proposition 1. *For $i = 1,2,3$, let $\tau_0,\tau_1,\lambda_0,\lambda_1,M$ as in table 1, let $I = D_{\tau_1}(\tau_0)$ and $J = D_{\lambda_1}(\lambda_0)$. Then for each (τ,λ) in $I\times J$, equation (21) has a unique solution $X(\tau,\lambda)$ in $B_r(\bar{X}(\tau,\lambda))$. Moreover, the map $(\tau,\lambda)\mapsto X = X(\tau,\lambda)$ is analytic and, for each real $\tau \in I$, a function X in $B\cap \ell^{-1}(J\hat{X})$ is a fixed point of F_τ if and only if $X = X(\tau,\lambda)$ for some real $\lambda \in J$, with $g(\tau,\lambda) = \ell_0 X(\tau,\lambda) = 0$.*

Figure 7 depicts the numerically computed zero level sets of the functions g obtained in proposition 1. Based on the images depicted in figure 7, one can guess that there are saddle-node bifurcations in each of the three cases being considered. We are left with the problem of understanding the bifurcation points in terms of the behavior of the zero level set of g. Following [28], a set of conditions sufficient for establishing the existence of a saddle-node bifurcation are given below. The interested reader is referred to [28] for the proof.

Lemma 2 (saddle-node bifurcation). *Let $I=[\tau_1,\tau_2]$ and $J=[b_1,b_2]$. Suppose that g is a real-valued C^3 function on the open neighborhood of $I\times J$, and let $\dot{g}$ and g' denote partial dedifferentiation with respect to the first and second argument, respectively.*

Assume that

(1) $g''>0$ *on* $I\times J$,
(2) $\dot{g}<0$ *on* $I\times J$,
(3) $g(\tau_1,0)\pm\frac{1}{2}bg'(\tau_1,0)>0$,
(4) $g(\tau_2,\pm b)>0$,
(5) $g(\tau_2,0)<0$.

Then the solution set of $g(\tau,\lambda)=0$ in $I\times J$ is the graph of a C^2 function $\tau=a(\lambda)$, defined on a proper subinterval J_0 of J. This function takes the value τ_2 at the endpoints of J_0, and satisfies $\tau_1<a(z_2)<\tau_2$ at all interior points of J_0, which includes the origin.

Finally, we establish the following lemma with computer assistance.

Lemma 3. *For $i=1,2,3$, consider the solution $X(\tau,\lambda)$ obtained in proposition 1. For any $X(\tau,\lambda)\in B_r(\bar{X}(\tau,\lambda))$ the function $g(\tau,\lambda)=\ell_0X(\tau,\lambda)$ if $i=1$ or $g(\tau,\lambda)=\ell_0X(\tau,-\lambda)$ if $i=2,3$ satisfies the assumptions of lemma 2.*

6. Gluing of branches

The next step is to follow the local branches established in the previous section away from the bifurcation point. For example, to prove theorem 2 it is necessary to establish that the solution branches B_1 and B_2 emerging from the saddle-node bifurcation at $\mu=0.199\,34\ldots$ continue smoothly all the way to the mass ratio $\mu=1/2$. More precisely, since lemma 3 establishes that the branches emerging from the saddle-node bifurcation extend up to $\mu=1633\cdot2^{-13}$, we want to show that the branches exist over the parameter interval $\mu\in\mathcal{I}=[1633\cdot2^{-13},1/2]$. This is done by numerically computing a high order Taylor expansion of K solution arcs on K sub-intervals of $\mathcal{I}$, proving the existence of a true solution near each of the numerical approximations using a fixed point argument, and showing that the sub-intervals 'glue together' in the proper way.

So, take $\{e_j\}$ again to be the basis introduced in the previous section, and expand the solution coefficients on each sub-interval as $\mathcal{X}$ Taylor polynomials in μ, given by

$$X_m(\mu)=\sum_j X_j^m(\mu)\,e_j,\quad X_j^m=\sum_{0\leqslant l\leqslant L_m}X_{jl}^m\left(\frac{\mu-\mu_m}{\tau_m}\right)^l, \tag{28}$$

where μ_m,τ_m, and L_m for $1\leqslant m\leqslant K$ are discussed further below. We numerically compute XT polynomials $\bar{X}_\mu^m$ for $1\leqslant m\leqslant K$ having that $\mathcal{F}_\mu(\bar{X}_\mu^m)\simeq\bar{X}_\mu^m$ for each m, and finite rank operators $M_\mu^m:\mathcal{X}\to\mathcal{X}$ such that $\mathbb{I}-M_\mu^m$ is an approximate inverse of $\mathbb{I}-D\mathcal{F}_\mu(\bar{X}_\mu^m)$ for each m.

As in the previous section, to use the Banach fixed point theorem we introduce new maps $\mathcal{G}_\mu^m$ as

$$\mathcal{G}_\mu^m(h)=\mathcal{F}_\mu(\bar{X}^m+\Lambda_\mu h)-\bar{X}^m+M_\mu^m h,\qquad \Lambda_\mu^m=\mathbb{I}-M_\mu^m,\qquad 1\leqslant m\leqslant K. \tag{29}$$

For $r>0$ and $w\in\mathcal{X}$, let $B_r(w)=\{v\in\mathcal{X}:\|v-w\|<r\}$ denote the ball of radius r about w. The branch B_1 (resp B_2) is partitioned into $K=59$ (resp. $K=63$) subintervals of various widths, chosen adaptively depending on how far we are from the bifurcation points. The

exact values of the centers μ_m and widths τ_m of the subintervals, as well as the degrees of the Taylor expansions and the numerically computed coefficients, are available in the data files `params.ads`, `run_b1.adb`, `run_b2.adb`. The following lemma is then established with computer assistance. See also section 7.

Lemma 4. *The following holds for each value of μ_m, τ_m, L_m in the data files mentioned above. For each $1 \leqslant m \leqslant K$ there exist a XT polynomial $\bar{X}^m(\mu)$ of degree L_m as described in (28), a bounded linear operator M_μ^m on $\mathcal{X}$, and positive real numbers ε_m, r_m, K_m satisfying $\varepsilon_m + K_m r_m < r_m$, such that*

$$\|\mathcal{G}_\mu^m(0)\| \leqslant \varepsilon_m, \quad \|D\mathcal{G}_\mu^m(Y)\| \leqslant K_m, \quad \forall Y \in B_{r_m}(0) \tag{30}$$

holds for all $\{\mu \in \mathbb{C} : |\mu - \mu_m| < \tau_m\}$.

So, in the case of the proof theorem 2, lemma 4 establishes the existence of 122 subbranches of ejection collision orbits. The next step is to check that the subbranches coincide at their endpoints, all the way to the saddle-node bifurcation. This is proven with computer assistance, by showing that the solutions match at the end points of the sub-branches. Then they are, in fact, pairwise on the same branch.

So, for each XT representation X_μ^m of an arc on the branch, let $P(X_\mu^m)$ be an enclosure of the image of the (x_2, y_2, p_2, q_2) components of X_μ^m, evaluated at $T = -1$.

Lemma 5. *Suppose that a pair of adjacent solution arcs X_μ^m, X_μ^{m+1} intersect at some value of $\bar{\mu}$, and assume that we have either*

$$P\left(X_\mu^m\right) \subset P\left(X_\mu^{m+1}\right) \text{ or } P\left(X_\mu^{m+1}\right) \subset P\left(X_\mu^m\right).$$

Then X_μ^m and X_μ^{m+1} represent different arcs on the same branch of ejection-collision solutions.

Repeated use of lemma 5 on each of the K subintervals completes the proof.

We still need to prove that the branches B_1 and B_2 are connected to the small branches emerging from the saddle-node bifurcation proved in lemma 3. To do so, let $\lambda_1 = 3/8 + B_{2^{-8}}(0)$ and $\lambda_2 = -343/512 + B_{2^{-8}}(0)$, with $B_r(0) = [-r, r]$. Let X_{sn} be the solution obtained in proposition 1 when $i = 1$, evaluated at $\mu = \bar{\mu} = 1633 \cdot 2^{-13}$, and let $P_j(X_{sn})$, $j = 1, 2$ be an enclosure of the value of the (x_2, y_2, p_2, q_2) components of X_{sn}, evaluated at $T = -1$, and $\lambda = \lambda_j$. Let $P_j(X_b)$, $j = 1, 2$, denote an enclosure of the values of the (x_2, y_2, p_2, q_2) components of the two solutions considered in lemma 4 corresponding to $\mu = \bar{\mu}$, evaluated at $T = -1$. Then the values $P_j(X_{sn})$ are an enclosure of a point of the solutions belonging to the branches connected to the saddle-node bifurcation, while the values $P_j(X_b)$ are an enclosure of a point of the solutions belonging to the larges branches.

Lemma 6. *For $i = 1, 2$*

$$P_j(X_b) \subset P_j(X_{sn}) \quad \text{and } P_1(X_b) \cap P_2(X_b) = \emptyset.$$

This implies that the two solutions obtained in lemma 5 at $\mu = \bar{\mu}$ are different, and coincide with the solutions obtained in proposition 1 and lemma 3. These results, together with the contraction mapping theorem and the implicit function theorem, imply theorem 2.

7. Computer representation and estimates

The computer assisted arguments discussed in sections 5 and 6 are implemented in the programming language Ada [29]. The remainder of the present section will serve as a rough guide for the reader interested in running these programs. The programs themselves are found at [30].

In the programs, many of the most important bounds are obtained by enclosing the ranges of functions. More precisely, the function $f\colon \mathcal{X} \to \mathcal{Y}$ is inclosed by a function F if assigning F to each set $X \subset \mathcal{X}$ of a given type (`Xtype`) a set $F(X) = Y \subset \mathcal{Y}$ of a given type (`Ytype`), in such a way that $y = f(x)$ belongs to Y for all $x \in X$. In Ada, such a bound F can be implemented by defining a `procedure F(X : in Xtype; Y : out Ytype)`.

We say that a number $x \in \mathbb{R}$ is representable if it can be expressed exactly as a floating point number in the computer. In our programs, a ball in a real Banach algebra $\mathcal{X}$ with unit $\mathbf{1}$ is represented using a pair `S = (S.C,S.R)`. Here `S.C` denotes a representable number (`Rep`) while `S.R` represents a nonnegative representable number (`Radius`). Then, for example, a ball in $\mathcal{X}$ is represented by the set $\langle \mathtt{S}, \mathcal{X} \rangle = \{x \in \mathcal{X} : \|x - (\mathtt{S.C})\mathbf{1}\| \leqslant \mathtt{S.R}\}$.

In the case that $\mathcal{X} = \mathbb{R}$, we refer to the data type just described by `Ball`. Numerical implementation of the enclosures of standard functions on the data type `Ball` are defined in the packages `Flts_Std_Balls`. The packages `Vectors` and `Matrices` extend the basic functions, facilitating the enclosure of vector and matrix valued functions. These kinds of data structures are used frequently in computer-assisted proofs, so we will describe only the more problem-specific features of our implementation.

In the present work, away from bifurcation points, one parameter families (i.e. branches) of solutions are described by one variable Taylor series. Two variable power series are used near bifurcation points. The one variable and two variable Taylor series are represented using data types called `Taylor1` and `Taylor2` respectively. These types consists of one and two variable power series, whose coefficients are of type `Ball`. Definitions, basic properties, and procedures are found in the packages `Taylors1` and `Taylors2` respectively. The interested reader will find these packages at [31].

Similarly, functions in $\mathcal{A}$ are represented using a type called `Cheb`, defined in a package called `Chebs`. This data type has coefficients in some Banach algebra with unit $\mathcal{X}$. For example, in the present work our `Cheb` objects have coefficients of either type `Taylor1` or `Taylor2`, depending on the application. The `Cheb` data type is represented by a triple `F = (F.C,F.E,F.R)`, with `F.C` an `array(0..K) of Ball`, `F.E` an `array(0..2*K) of Radius`, and `F.R` an object of type `Radius`. The later describes the ellipse of analyticity on which the functions in $\mathcal{A}$ are defined. That is $\mathtt{F.R} = 5/4$. The set $\langle \mathtt{F}, \mathcal{A} \rangle$ consists of function $u = p + h \in \mathcal{A}$ with

$$p(t) = \sum_{j=0}^{K} \langle \mathtt{F.C(J)}, \mathcal{X} \rangle T_j(t), \qquad h = \sum_{j=0}^{2K} h^j, \qquad h^j(t) = \sum_{m \geqslant j} h^j_m T_m(t).$$

Here $\|h^J\| \leqslant \mathtt{F.E(J)}$, for all J.

The operations needed in our proof are bound efficiently using these enclosures. The data types `Chebs` and `Taylors1` are used to define the type `XX`, which is in turn used to represent the subspaces $\mathbb{P}_{\{j\}}\mathcal{A}_{\mathcal{B}}$ (coefficient modes) and $\mathbb{P}_{\{j,j+1,\ldots\}}\mathcal{A}_{\mathcal{B}}$ (error modes). Partitions of unity (in the sense of direct sums) are defined using Arrays of `CylinderMode`. The procedure `Make` implements these partitions for the spaces $\mathcal{A}_j$ described in section 6.

Operations needed in the implementation of a Newton-like operator are defined in the higher level packages `Linear` and `Linear.Contr`, which have been used to solve a wide variety of problems. The procedures defined in these packages are designed to work with generic function

types `Fun`, as long as their associated `Modes` are specified. In the present work, these packages are used to implement quasi-Newton maps $\mathcal{N}$, estimate derivatives (such as the linear operator such as $D\mathcal{N}(h)$) and to check contraction bounds like those in (27) and (30). A much more complete description of of the package `Modes` is found for example in [32, 33].

Data availability statement

All data that support the findings of this study are included within the article (and any supplementary files).

Appendix. Remarks on the literature

The first computer assisted proofs dealing with the dynamics of the planar CRTBP appeared in the papers [34, 35] by the first author, and established the existence of branches of periodic orbits, as well as chaotic subsystems with positive topological entropy for the CRTBP with equal masses. Shortly thereafter, Wilczak and Zgliczyński generalized these techniques to prove the existence of heteroclinic connections between periodic orbits in the Sun–Jupiter system [36, 37].

Over the last 20 years, many additional theorems have been proven for planar and spatial CRTBPs using computer assisted arguments. Rather than attempting a systematic review, we refer the interested reader to section 1.3 of [12], where a more thorough discussion and many additional references are found. We also mention the general review article of van den Berg and Lessard [38] on computer assisted methods of proof in dynamical systems theory, and the review of Gómez-Serrano [39] on computer assisted proofs for PDEs. Undergraduate and graduate level discussions of validated numerical techniques, appropriate for use in computer assisted proofs, are found in the book of Tucker [40], in the review article of Rump [41], and also in the monograph of Nakao *et al* [42].

A central question in nonlinear analysis is to understand the dependence of solutions on problem parameters. Given the importance of the question, it is natural that a number of authors have devoted substantial effort to the development of computer assisted methods of proof for continuation and bifurcation arguments. Perhaps the first computer assisted result of this kind was the Paper of Plum [43] on continuation of branches of solutions of one parameter families of second order scalar BVPs. Computer assisted proofs for bifurcations in the Rayleigh–Bénard problem, using similar techniques, were given by Nakao, Watanabe, Yamamoto, Nishida, and Kim in [44].

The paper [28], by Koch and the first author, provides a coherent example of how techniques of validated continuation can be combined with mathematically rigorous bifurcation analysis to obtain mathematically rigorous bifurcation diagrams. The authors studied equilibrium solutions for a one parameter family of scalar PDEs defined on a one dimensional spatial domain with Dirichlet boundary conditions. An example application to a scalar PDE defined on a two dimensional spatial domain with periodic boundary conditions was given by van den Berg and Williams in [45]. For other extensions and applications of validated continuation we refer to the papers of Day *et al* [46], Gameiro *et al* [47], and to the references therein.

More recently, Gazzola, Koch and the first author developed a computer assisted continuation methods based on a single variable Taylor expansion for branches of solutions of nonlinear problems. See [27] for an application to the planar Navier–Stokes equation. The authors set up the continuation problem as a fixed point problem on a bigger Banach space, and solve 'all-at-once' for a high order expansion of the branch using any desired basis functions. A

similar all-at-once set up, employing a multi-variable Taylor expansion of a suitable normal form, is used to prove the existence of pitchfork bifurcations. The approach of the paper just cited is the basis of the high order continuation and bifurcation results of the present work.

Breden and Kuehn developed a similar computer assisted continuation method using general expansions for branches of solutions of nonlinear problems [48, 49] (not just Taylor). The idea behind their work just cited is that, when studying random perturbations of differential equations, it is important to expand the branch using basis functions adapted to the distribution of the noisy parameter. We also mention the recent work of Calleja *et al* the second author in [50], where the existence of a global branch of choreographic solutions is established using computer assisted methods of proof. The branch of periodic orbits are expressed using Fourier–Chebyshev series. More precisely, each choreography along the branch is represented by a Fourier series and the dependence of the branch the parameter is represented by a Chebyshev series (rather than multiple Taylor series as in the present work). One quarter of the global branch of solutions is obtained using a single Chebyshev domain, and the remainder of the global branch is obtained by a symmetry argument.

We also mention the work of Walawska and Wilczak [51], where the authors use computer assisted continuation and bifurcation arguments to study families of periodic orbits in the spatial CRTBP. More than this, they follow a family of out-of-plane periodic orbits from a symmetry breaking bifurcation, through a number of secondary bifurcations, and back to where it began. That is, they prove the existence of a closed circle- or global family—of periodic orbits locally parameterized by energy (note that a circle of periodic orbits is topologically a torus). Note also that in the work of [12], already mentioned above, the authors prove theorems on the existence of one parameter families of periodic orbits—parameterized by energy—which 'pass through' collision.

As a final remark we note that while the present work and [12] both deal with computer assisted existence proofs for ejection–collision orbits, the two works have very different agendas and there are important differences in their approaches. In particular, the results of [12] focus on fixed values of the mass ratio and energy. The results are based on the study of certain multiple shooting problems formulated in $\mathbb{R}^d$ (usually with d large). *A-posteriori* analysis of these shooting problems requires only the application of an elementary finite dimensional Newton–Kantorovich argument. The techniques lead to transversality of the results, leading to only local information about the existence of branches.

The goal of that work was to develop 'plug and play' shooting templates, suitable for a wide variety of computer assisted proofs involving any number of collision or near collision events. Because of this, all infinite dimensional complications are hidden behind the sophisticated CAPD library for computing mathematically rigorous set enclosures of solutions to initial value problems and variational equations. An excellent overview of the CAPD library, with many worked examples and a wealth of additional references is found in the review article of Kapela *et al* [52].

Alternatively, the present work formulates a single fixed point equation describing an ejection–collision orbit or a branch of ejection–collision orbits in an appropriate product of function spaces. The advantage of the functional analytic approach in the present context is that the problem parameters appear in the fixed point operator in a completely explicit way, rather than entering the problem implicitly through flow map as in [12]. This set-up facilitates high order approximation of solution branches using techniques discussed in section 5. The proofs exploits software libraries developed by Hans Koch and the first author over the course of the last 20 years. See for example the works of [31–33], and also the references discussed therein as this list is by no means exhaustive.

ORCID iDs

Gianni Arioli https://orcid.org/0000-0002-3646-7900
J D Mireles James https://orcid.org/0000-0001-8449-9408

References

[1] Guardia M, Kaloshin V and Zhang J 2019 Asymptotic density of collision orbits in the restricted circular planar 3 body problem *Arch. Ration. Mech. Anal.* **233** 799–836
[2] Chazy J 1922 Sur l'allure du mouvement dans le problème des trois corps quand le temps croît indéfiniment *Ann. Sci. École Norm. Sup.* **39** 29–130
[3] Poincaré H 1993 Periodic and asymptotic solutions *New Methods of Celestial Mechanics Vol. 1* (*History of Modern Physics and Astronomy* vol 13) (American Institute of Physics) (Translated from the French, Revised reprint of the 1967 English translation, With endnotes by V. I. Arnold, Edited and with an introduction by Daniel L. Goroff)
[4] Poincaré H 1993 *New Methods of Celestial Mechanics Vol. 2* (*History of Modern Physics and Astronomy* vol 13) (American Institute of Physics) (Approximations by series, Translated from the French, Revised reprint of the 1967 English translation, With endnotes by V. M. Alekseev, Edited and with an introduction by Daniel L. Goroff)
[5] Poincaré H 1993 Integral invariants and asymptotic properties of certain solutions *New Methods of Celestial Mechanics Vol. 3* (*History of Modern Physics and Astronomy* vol 13) (American Institute of Physics) (Translated from the French, Revised reprint of the 1967 English translation, With endnotes by G. A. Merman, Edited and with an introduction by Daniel L. Goroff)
[6] Levi-Civita T 1920 Sur la régularisation du problème des trois corps *Acta Math.* **42** 99–144
[7] Szebehely V 1967 *Theory of Orbits* (Academic Inc)
[8] Celletti A 2006 Basics of regularization theory *Chaotic Worlds: from Order to Disorder in Gravitational N-Body Dynamical Systems* ed B A Steves A J Maciejewski and M Hendry (Springer) pp 203–30
[9] Ollé M, Rodríguez O and Soler J 2021 Transit regions and ejection/collision orbits in the RTBP *Commun. Nonlinear Sci. Numer. Simul.* **94** 105550
[10] Ollé M, Rodríguez O and Soler J 2020 Analytical and numerical results on families of *n*-ejection-collision orbits in the RTBP *Commun. Nonlinear Sci. Numer. Simul.* **90** 105294
[11] M-Seara T, Ollé M, Rodríguez O and Soler J 2023 Generalized analytical results on *n*-ejection-collision orbits in the RTBP. Analysis of bifurcations *J. Nonlinear Sci.* **33** 17
[12] Maciej J C, Kepley S and James J D M 2023 Computer assisted proofs for transverse collision and near collision orbits in the restricted three body problem *J. Differ. Equ.* **366** 132–91
[13] Llibre J 1982 On the restricted three-body problem when the mass parameter is small *Celest. Mech.* **28** 83–105
[14] Lacomba E A and Llibre J 1988 Transversal ejection-collision orbits for the restricted problem and the Hill's problem with applications *J. Differ. Equ.* **74** 69–85
[15] Meyer K R, Hall G R and Offin D 2009 *Introduction to Hamiltonian Dynamical Systems and the N-Body Problem* (*Applied Mathematical Sciences* vol 90) 2nd edn (Springer)
[16] Capiński M and Pasiut A 2024 Oscillatory collision approach in the earth-moon restricted three body problem (arXiv:2401.12386)
[17] Darwin G H 1897 Periodic orbits *Acta Math.* **21** 99–242
[18] Strömgren E 1934 Connaissance actuelle des orbites dans le probleme des trois corps *Bull. Astron.* **9** 87–130
[19] Moulton F R, Buchanan D, Buck T, Griffin F L, Longley W R and MacMillan W D 1920 *Periodic Orbits* vol 161 (Carnegie Institution of Washington)
[20] Muñoz Almaraz F J, Freire E, Galán J, Doedel E and Vanderbauwhede A 2003 Continuation of periodic orbits in conservative and Hamiltonian systems *Physica* D **181** 1–38
[21] Doedel E J, Romanov V A, Paffenroth R C, Keller H B, Dichmann D J, Galán-Vioque J and Vanderbauwhede A 2007 Elemental periodic orbits associated with the libration points in the circular restricted 3-body problem *Int. J. Bifurcation Chaos* **17** 2625–77
[22] Doedel E J, Paffenroth R C, Keller H B, Dichmann D J, Galán-Vioque J and Vanderbauwhede A 2003 Computation of periodic solutions of conservative systems with application to the 3-body problem *Int. J. Bifurcation Chaos* **13** 1353–81

[23] Calleja R C, Doedel E J, Humphries A R, Lemus-Rodríguez A and Oldeman E B 2012 Boundary-value problem formulations for computing invariant manifolds and connecting orbits in the circular restricted three body problem *Celest. Mech. Dynam. Astronom.* **114** 77–106
[24] Simo C 1990 On the analytical and numerical approximation of invariant manifolds *Modern Methods in Celestial Mechanics, Comptes Rendus de la 13ieme Ecole Printemps d'Astrophysique de Goutelas (France), 24-29 Avril, 1989*, ed D Benest and C Froeschle (edns Frontieres) p 285
[25] Doedel E J 2000 Lecture notes on numerical analysis of bifurcation problems *International Course on Bifurcations and Stability in Structural Engineering* (Université Pierre et Marie Curie)
[26] Kuznetsov Y A 2023 *Elements of Applied Bifurcation Theory* (*Applied Mathematical Sciences* vol 112) 4th edn (Springer)
[27] Arioli G, Gazzola F and Koch H 2021 Uniqueness and bifurcation branches for planar steady Navier–Stokes equations under Navier boundary condition *J. Math. Fluid Mech.* **23** 49
[28] Arioli G and Koch H 2010 Computer-assisted methods for the study of stationary solutions in dissipative systems, applied to the Kuramoto–Sivashinski equation *Arch. Rational Mech. Anal.* **197** 1033–51
[29] ISO/IEC 8652:2012(e) *Ada reference manual* (International Organisation for Standardization)
[30] Gianni A and J D M 2024 Programs and data files for the proof of lemmas 1,3,4,5,6 (https://arioli.faculty.polimi.it/Section7.tar.gz)
[31] Arioli G 2022 Computer assisted proof of branches of stationary and periodic solutions and hopf bifurcations, for dissipative PDEs *Commun. Nonlinear Sci. Numer. Simul.* **105** 106079
[32] Arioli G and Koch H 2019 Non-radial solutions for some semilinear elliptic equations on the disk *Nonlinear Anal.* **179** 294–308
[33] Arioli G and Koch H 2020 Traveling wave solutions for the FPU chain: a constructive approach *Nonlinearity* **33** 1705–22
[34] Arioli G 2002 Periodic orbits, symbolic dynamics and topological entropy for the restricted 3-body problem *Commun. Math. Phys.* **231** 1–24
[35] Arioli G 2004 Branches of periodic orbits for the planar restricted 3-body problem *Discrete Contin. Dyn. Syst.* **11** 745–55
[36] Wilczak D and Zgliczynski P 2003 Heteroclinic connections between periodic orbits in planar restricted circular three-body problem—a computer assisted proof *Commun. Math. Phys.* **234** 37–75
[37] Wilczak D and Zgliczyński P 2005 Heteroclinic connections between periodic orbits in planar restricted circular three body problem. II *Commun. Math. Phys.* **259** 561–76
[38] van den Berg J B and Lessard J P 2015 Rigorous numerics in dynamics *Not. Amer. Math. Soc.* **62** 1057–61
[39] Gómez-Serrano J 2019 Computer-assisted proofs in PDE: a survey *SeMA J.* **76** 459–84
[40] Tucker W 2011 A short introduction to rigorous computations *Validated Numerics* (Princeton University Press)
[41] Siegfried M R 2010 Verification methods: rigorous results using floating-point arithmetic *Acta Numer.* **19** 287–449
[42] Nakao M T, Plum M and Watanabe Y 2019 *Numerical Verification Methods and Computer-Assisted Proofs for Partial Differential Equations* (*Springer Series in Computational Mathematics* vol 53) (Springer)
[43] Plum M 1995 Existence and enclosure results for continua of solutions of parameter-dependent nonlinear boundary value problems *J. Comput. Appl. Math.* **60** 187–200
[44] Nakao M T, Watanabe Y, Yamamoto N, Nishida T and Kim M-N 2010 Computer assisted proofs of bifurcating solutions for nonlinear heat convection problems *J. Sci. Comput.* **43** 388–401
[45] van den Berg J B and Williams J F 2017 Validation of the bifurcation diagram in the 2D Ohta-Kawasaki problem *Nonlinearity* **30** 1584–638
[46] Day S, Lessard J-P and Mischaikow K 2007 Validated continuation for equilibria of PDEs *SIAM J. Numer. Anal.* **45** 1398–424
[47] Gameiro M, Lessard J-P and Mischaikow K 2008 Validated continuation over large parameter ranges for equilibria of PDEs *Math. Comput. Simul.* **79** 1368–82
[48] Breden M and Kuehn C 2020 Computing invariant sets of random differential equations using polynomial chaos *SIAM J. Appl. Dyn. Syst.* **19** 577–618
[49] Breden M 2023 A posteriori validation of generalized polynomial chaos expansions *SIAM J. Appl. Dyn. Syst.* **22** 765–801

[50] Calleja R, García-Azpeitia C, Hénot O, Lessard J-P and James J D M 2024 From the Lagrange triangle to the figure eight choreography: proof of Marchal's conjecture (arXiv:2406.17564 [math.DS])

[51] Walawska I and Wilczak D 2019 Validated numerics for period-tupling and touch-and-go bifurcations of symmetric periodic orbits in reversible systems *Commun. Nonlinear Sci. Numer. Simul.* **74** 30–54

[52] Kapela T, Mrozek M, Wilczak D and Zgliczyński P 2020 CAPD::DynSys: a flexible C++ toolbox for rigorous numerical analysis of dynamical systems *Commun. Nonlinear Sci. Numer. Simul.* **101** 105578